

# Gamma-ray absorption in the massive TeV Binary LS 5039

Author: Núria Casasayas Barris

Facultat de Física, Universitat de Barcelona, Diagonal 645, 08028 Barcelona, Spain.

Advisor: Marc Ribó

**Abstract:** The recent detections of binary systems emitting very high-energy (VHE) gamma-rays has introduced a new class of binaries: gamma-ray binaries. These binaries, composed of a compact object and a massive star, are distinguished by a non-thermal emission with a peak above 1 MeV in the spectral energy distribution (SED). For massive companions with effective temperature of 20 000–40 000 K, the stellar photon energies are in the range for pair-production with TeV photons. Therefore, the VHE emission can be efficiently absorbed. The absorption is modulated due to its dependence on the orbital geometry because of the angular dependence of the pair production cross-section and the energy threshold. We show that the total cross-section is energy dependent, and for  $T_* = 39\,000$  K the  $\gamma$ -ray photons with hundreds of GeV are highly absorbed. We have written a Fortran code to perform numerical calculations of the opacity of the  $\gamma$ -ray absorption due to pair production for the  $\gamma$ -ray binary LS 5039, considering the point-like approximation for the companion. The results obtained for a system inclination  $i = 60^\circ$  show the minimum absorption when the compact object is far from the star and close to the observer, and the maximum near the periastron. Our results are compared with Dubus (2006), where a complete treatment considering the massive star size is shown, finding minor differences. We also compare the available VHE lightcurve with a transmission lightcurve at 3 TeV and conclude that the absorption due to pair production is insufficient to explain the observations, implying that cascading or emission away from the compact object have to be invoked.

## I. INTRODUCTION

The new generation of observatories in the mid-2000s enabled the discovery of binary systems emitting high-energy (HE, 0.1–100 GeV) or very high-energy (VHE > 100 GeV) gamma-rays (see Dubus 2013 and references therein). A new class of binaries has emerged, called “gamma-ray binaries”, composed of a neutron star or a black hole in orbit around a massive star and distinguished by their non-thermal emission peak above 1 MeV in the spectral energy distribution (SED)  $F_\nu \nu$ . There is also a strong contribution to the SED from the luminous massive star, but this is easily separated from the non-thermal continuum as it is thermal emission with a maximum temperature of a few eV.

Currently, the five following gamma-ray binary systems are known: PSR B1259–63, the first binary to be detected at VHE gamma-rays in 2004 by Aharonian et al. (2005a); LS 5039, followed in 2005 (Aharonian et al. 2005b); LS I +61°303, the third gamma-ray binary detected at VHE gamma-rays by Albert et al. (2006); HESS J0632+057, found as a point-like source in the H.E.S.S. study of the Galactic Plane (Aharonian et al. 2007); and 1FGL J1018.6–5856, found in a search for periodic flux variations from *Fermi*/LAT sources (Fermi LAT Collaboration et al. 2012). The detection of  $\gamma$ -ray binaries initiated a debate as if the high-energy emission was due to accretion energy released in the form of a relativistic jet (microquasar scenario) or due to rotational energy released as a pulsar wind (pulsar scenario). A sketch of both scenarios is presented in Fig. 1. In the microquasar scenario the compact object accretes matter from the stellar wind of the massive companion and/or

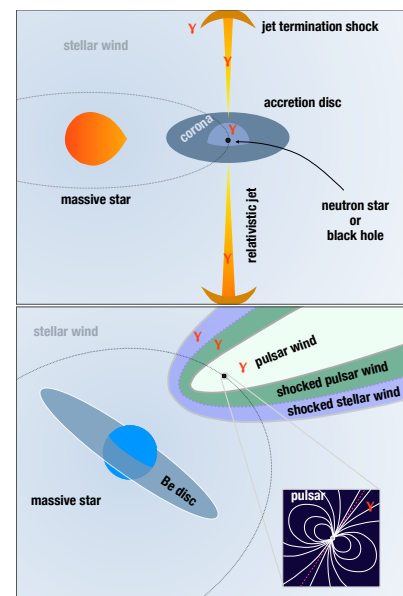


FIG. 1: Scenarios for gamma-ray emitting binaries: microquasar (top), pulsar (bottom). From Dubus (2013).

Be disc (if present). Part of the energy released in the accretion disc is used to launch a relativistic jet. Gamma-ray emission can arise from the corona of the accretion disc, within the jet, or at the terminal shock of the jet. On the other hand, in the pulsar scenario the relativistic wind from the rotation-powered pulsar interacts with the stellar wind and/or Be disc of the companion. Gamma-ray emission can occur near the pulsar, within the pulsar wind, or at the shocks terminating the pulsar and stellar

wind. PSR B1259–63 is at present the only  $\gamma$ -ray binary in which the scenario, pulsar in this case, is proven. LS 5039 seems to behave as expected in the pulsar scenario although radio pulsations have not been detected (Moldón et al. 2012).

The large luminosity of the companion star provides an abundant source of seed photons for inverse Compton scattering with HE particles. At the same time, the dense radiation field can absorb VHE  $\gamma$ -ray emission through pair production  $\gamma\gamma \rightarrow e^+e^-$  (Gould & Schröder, 1967). With stellar effective temperatures in the 20 000–40 000 K range, the typical target photon energy is a few eV, which is in the energy range for pair production with TeV photons. The  $\gamma\gamma$  opacity due to pair production depends strongly on the geometry. The absorption will vary depending upon the relative location of the source of  $\gamma$ -rays, the companion star and the observer because of the angular dependence of the pair production cross-section and the energy threshold. If  $\gamma$ -ray emission is isotropic and close to the compact object, absorption will be periodically modulated in a predictable way.

Here, absorption light-curves for  $\gamma$ -ray emission close to the compact object are examined for LS 5039 using the measured orbit and taking into account the point-like approximation for the massive star (for the complete treatment see Dubus 2006). The results are compared with the LS 5039 H.E.S.S. data and the differences between them are discussed.

## II. GAMMA-RAY ABSORPTION

As discussed above,  $\gamma$ -ray emission can be absorbed by the dense radiation field through pair production. This absorption of a  $\gamma$ -ray of energy  $E$  on a stellar photon of energy  $\epsilon$  occurs above an energy threshold given by Gould & Schröder (1967):

$$\epsilon E \geq \frac{2m_e^2 c^4}{(1 - \mathbf{e}_\gamma \mathbf{e}_\star)} \quad (1)$$

where  $\mathbf{e}_\gamma$  is a unit vector along the direction of propagation of the  $\gamma$ -ray and  $\mathbf{e}_\star$  is the unit vector along the direction of propagation of the stellar photon (see Fig. 2).

Absorption only occurs when the stellar photons are at an angle to the  $\gamma$ -ray smaller than  $\pi$ , and the minimum  $\epsilon E$  (energy threshold) occurs for head-on collisions. Thus, we can see that  $\gamma$ -rays propagating directly away from the source of target photons (star) are not absorbed.

On the other hand, the location of maximum absorption changes as the compact object revolves around the massive star. Assuming isotropic emission close to the compact object in a small region compared to the binary size, the resulting absorption lightcurve of a given energy depends on the orbital parameters (orbital period  $P_{\text{orb}}$ , total mass  $M$ , eccentricity  $e$ , argument of periastron  $\omega$  and inclination  $i$ ). We note that absorption is invariant of orbital phase only for circular orbits as seen from

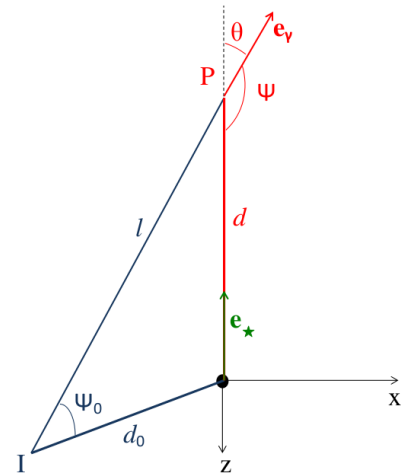


FIG. 2: Geometry for absorption of a  $\gamma$ -ray at location P due to pair production with stellar photons emitted at the assumed point-like star (at origin). The  $\gamma$ -ray is emitted at I and  $l$  is the length of the  $\gamma$ -ray path to P. The  $(x,z)$  plane is defined by the star and the  $\gamma$ -ray path. Adapted from Dubus (2006).

above ( $i = 0^\circ$ ,  $e = 0$ ). For inclined and circular orbits the lightcurves are symmetric with respect to the orbital phase of superior or inferior conjunction. In an eccentric orbit the absorption varies even with  $i = 0^\circ$ .

The differential absorption opacity seen by a  $\gamma$ -ray of energy  $E$  emitted close to the compact object (I) and located at P, travelling in the direction  $\mathbf{e}_\gamma$  due to stellar photons of energy  $\epsilon$  emitted at the star along  $\mathbf{e}_\star$ , considering the point source approximation ( $R_\star \ll d$ ;  $1 - \mathbf{e}_\gamma \mathbf{e}_\star = 1 + \cos \psi$ ) is, following Dubus 2006:

$$d\tau_{\gamma\gamma} = \pi \left( \frac{R_\star}{d} \right)^2 \sigma_{\gamma\gamma} n_\epsilon (1 + \cos \psi) dl d\epsilon \quad (2)$$

where  $\sigma_{\gamma\gamma}$  is the  $\gamma\gamma$  cross-section and  $n_\epsilon$  is the energy distribution of the target photons. The star is assumed to have a black body radiation density with a temperature  $T_\star$ :

$$n_\epsilon = \frac{2\epsilon^2}{h^3 c^3} \frac{1}{\exp(\epsilon/kT_\star) - 1} \text{ ph cm}^{-3} \text{ erg}^{-1} \text{ sr}^{-1} \quad (3)$$

Therefore, the absorption depends on  $n_\epsilon$ : VHE  $\gamma$ -rays are able to interact with the Rayleigh-Jeans tail while lower energy  $\gamma$ -rays interact with the Wien part.

Considering the collision between a VHE photon ( $E$ ) and a low-energy photon ( $\epsilon$ ) in the laboratory system in which the high-energy photon is moving along a given axis in the positive direction and the low-energy photon is moving in a direction making an angle  $\theta$  with the given axis (see Fig. 2), it can be found in Gould & Schröder (1967) that the total cross-section of the process is

$$\sigma_{\gamma\gamma} = \frac{1}{2} \pi r_0^2 (1 - \beta^2) [(3 - \beta^4) \ln \frac{1 + \beta}{1 - \beta} - 2\beta(2 - \beta^2)] \quad (4)$$

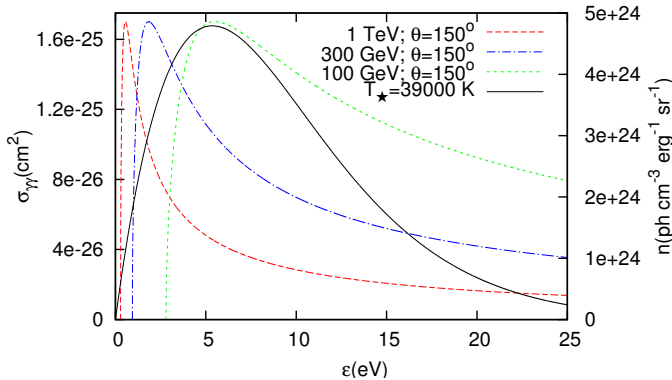


FIG. 3: Dependence of the total  $\gamma\gamma$  cross-section with stellar photon energy for  $\theta = 150^\circ$  (left axis). The long-dashed (red) line is for 1 TeV  $\gamma$ -ray photon, the dot-dashed (blue) for a 300 GeV photon and the short-dashed (green) for a 100 GeV photon. The black body radiation density (right axis) for an effective temperature  $T_\star = 39000$  K is also shown (black solid line).

where  $r_o = e^2/mc^2$  is the classical electron radius. The relation between  $\beta$  and  $E$ ,  $\epsilon$  and  $\theta$  is obtained with the invariant total energy-momentum for the two photons:

$$2\epsilon E(1 - \cos\theta) = 4E_e^2 \quad (5)$$

where  $E_e$  is the electron (positron) total energy in the center of masses. Following Nikishov 1962, we define

$$s = \left(\frac{E_e}{mc^2}\right)^2 = \left(\frac{\epsilon E}{2m^2c^4}\right)(1 - \cos\theta); \quad \beta = (1 - 1/s)^{1/2} \quad (6)$$

Note that  $\psi = \pi - \theta$  (see Fig. 2).

Therefore, the total cross-section is energy dependent. For a star with  $T_\star = 39000$  K,  $\gamma$ -ray photons with energies of hundreds of GeV are efficiently absorbed, as we show in Fig. 3.

On the other hand, the length  $l$  of the  $\gamma$ -ray path since its emission at a distance  $d_0$  from the star and at an angle  $\psi_0$  (see Fig. 2) to P where the  $\gamma$ -ray photon is absorbed, is related to  $\psi$  with:

$$\psi = \tan^{-1}\left(\frac{d_0 \sin \psi_0}{d_0 \cos \psi_0 - l}\right) \quad \text{for } l < d_0 \cos \psi_0 \quad (7)$$

$$\psi = \pi + \tan^{-1}\left(\frac{d_0 \sin \psi_0}{d_0 \cos \psi_0 - l}\right) \quad \text{for } l > d_0 \cos \psi_0 \quad (8)$$

The distance  $d$  from the star to P, where the  $\gamma$ -ray is absorbed, is defined as

$$d^2 = d_0^2 + l^2 - 2d_0l \cos \psi_0 \quad (9)$$

Finally,  $\cos \psi_0 = \sin \alpha \sin i$ , being  $\alpha = V + \omega$  and  $V$  the orbit true anomaly.

This deduction is used to estimate the opacity to infinity for a  $\gamma$ -ray of given energy  $E$ :

$$\tau_{\gamma\gamma} = \int_0^\infty dl \int_{\epsilon_{min}}^\infty \frac{d\tau_{\gamma\gamma}}{d\epsilon dl} d\epsilon \quad (10)$$

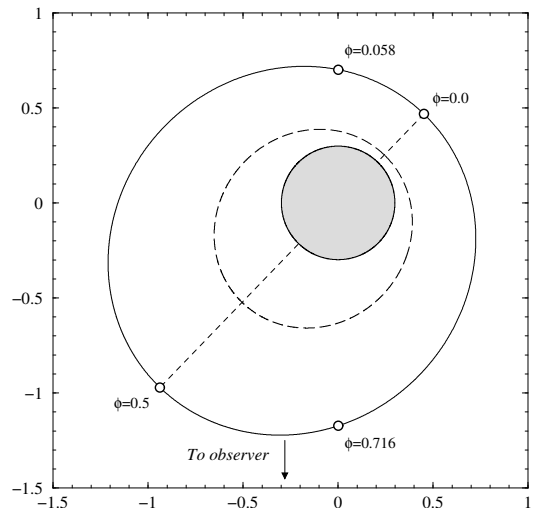


FIG. 4: Orbit of LS 5039 seen from above,  $i = 0^\circ$ . The axis units are semimajor axes. The observer is located at the bottom of the figure and the numbers refer to the orbital phase. It is shown the periastron ( $\phi_{\text{per}} = 0$ ), the superior conjunction ( $\phi_{\text{sup}} = 0.058$ , when the compact object passes behind of the massive star as seen by observer) and the inferior conjunction ( $\phi_{\text{inf}} = 0.716$ , when the compact object passes in front of the star). Figure from Casares et al. (2005).

The threshold is  $\epsilon_{min} = 2m_e^2c^4/E(1 + \cos\psi)$ . It is convenient to rewrite the  $\gamma$ -ray path ( $l$ ) integral as a definite integral on  $\psi$  within the interval  $[\psi_0, \pi]$ , and the energy integral as a definite integral on  $\beta$  between  $[0, 1]$ .

### III. APPLICATION TO LS 5039

#### A. LS 5039

LS 5039 was identified in 1997 as a massive X-ray binary system, and radio emission was discovered in 1998. It had been suspected for a long time that this object could emit high energy radiation up to the VHE  $\gamma$ -ray domain (Paredes et al. 2000). In 2004, during the H.E.S.S. Galactic plane scan, VHE emission from LS 5039 was discovered (Aharonian et al. 2005b).

LS 5039 is a binary system located at  $\sim 2.5$  kpc in the southern Milky Way, and it belongs to the Scutum constellation. It is composed of a luminous O6.5V star and an unknown compact object, a black hole or a neutron star, and has an orbital period of 3.9 days and an excentricity  $e \approx 0.35$ . The properties of the O6.5V star are:  $L_\star \approx 2 \times 10^5 L_\odot$ ,  $T_\star = 39000$  K,  $R_\star \approx 9.3R_\odot$  and  $M_\star \approx 23M_\odot$  (Casares et al. 2005). At periastron, the compact object is only  $\sim 1R_\star$  away from the surface of the star and the argument of periastron is  $\omega \approx 226^\circ$  for the companion and  $\approx 46^\circ$  for the compact object (see Fig. 4).

The orbit inclination relative to the plane of the sky has not been fully established yet. Taking into account the

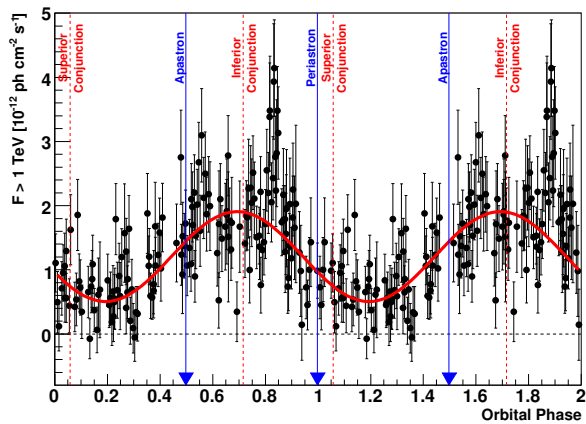


FIG. 5: Integral  $\gamma$ -ray flux above 1 TeV as function of orbital phase of LS 5039 from H.E.S.S. data taken in 2004 and 2005. Two periods are shown. The blue arrows indicate the phases of maximum (apastron) and minimum (periastron) binary separation. The dashed red lines show the phases of superior and inferior conjunction. The red line represents a sinusoidal fit to the data. From Aharonian et al. (2006).

mass function and the more conservative constraints on the system inclination two orbital solutions are adopted to illustrate the extremes:  $i = 60^\circ$  corresponding to a canonical  $1.4M_\odot$  neutron star and  $i = 20^\circ$ , corresponding to a  $4.5M_\odot$  black hole.

The 2004 observations of LS 5039 by H.E.S.S. were followed up in 2005, leading a total dataset of 69.2 hours of observation. To optimize the coverage over the orbit, the observations were spread over more than six months, resulting in a wide range of observations conditions. The observations are in a threshold varying between  $\sim 100$  GeV and  $\sim 1$  TeV. We show in Fig. 5 the integral  $\gamma$ -ray flux above 1 TeV as a function of orbital phase ( $\phi$ ) (Aharonian et al. 2006). The behaviour is approximately sinusoidal. The bulk of the emission is confined in the  $\phi \sim 0.45$ – $0.9$  interval, which is approximately half of the orbital cycle. The emission minimum is at  $\phi \sim 0.2$  a bit further than superior conjunction which is at  $\phi \sim 0.058$ . The maximum VHE flux is at  $\phi \sim 0.7$ , which is near inferior conjunction ( $\phi \sim 0.716$ ), where the compact object is in front of the massive star.

## B. Gamma-ray absorption in LS 5039

Here, results of the orbital modulation of  $\gamma$ -ray absorption in LS 5039 considering the point-like approximation for the massive star are shown. We have written a Fortran code to compute the integral of the opacity, using the trapezoidal method, and to obtain the  $\gamma$ -ray transmission  $\exp(-\tau_\gamma)$ . We show in Fig. 6 the results for the  $i = 60^\circ$  case. The minimum absorption (peak transmission) is predicted at  $\phi \sim 0.6$ , when the compact object is far from the massive star and close to the observer (see Fig. 4). The maximum absorption occurs at  $\phi \sim 0.1$ , near

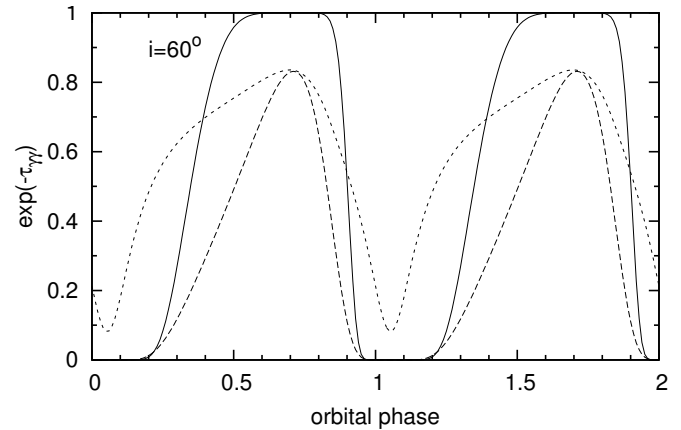


FIG. 6: Results obtained of the  $\gamma$ -ray transmission curve in LS 5039 for a system inclination  $i = 60^\circ$ . The solid line is for 100 GeV photons (H.E.S.S. threshold), long-dashed is for 1 TeV and short-dashed for 10 TeV. Periastron is at  $\phi = 0$ .

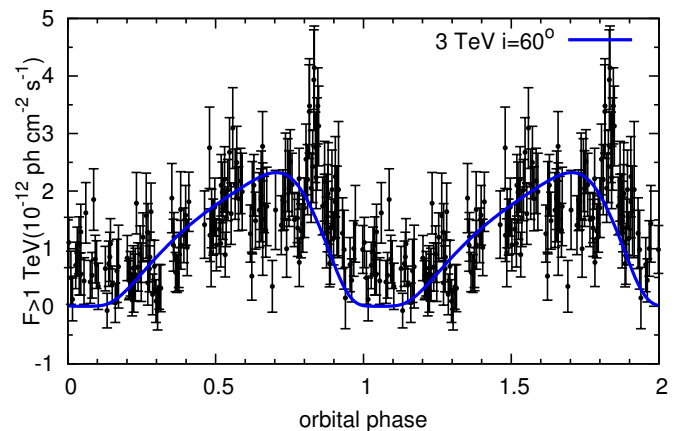


FIG. 7: Integral  $\gamma$ -ray flux above 1 TeV as function of orbital phase of LS 5039 from H.E.S.S. data. The blue line corresponds to the transmission curve for a 3 TeV  $\gamma$ -ray photon and  $i = 60^\circ$  scaled by a factor 3.

the periastron. In the case of  $i = 20^\circ$  the absorption is higher and the transmission variability more symmetric. Dubus 2006 conducted the same study but considering the finite size of the star. The main difference between both methods is visible for 10 TeV at  $\phi \sim 0$  because for lower energies the opacity is very high and therefore, the transmission very low (see Fig. 2 from Dubus 2006). This difference is because, considering the star size the star regions which are at a smaller angle to the observer (seen from the compact object) present a lower energy threshold, in contrast to larger angles. However, globally, that produces a decrease in the threshold, resulting in a higher absorption (lower transmission) than our results.

We show in Fig. 7 the transmission lightcurve at 3 TeV for an inclination of  $60^\circ$  superimposed to the H.E.S.S. lightcurve. The general trend is reproduced, but null transmission is expected at superior conjunction while significant flux is detected.

## IV. DISCUSSION

We have shown that the VHE emission from LS 5039 is orbitally modulated. However, the signal observed by H.E.S.S. at  $\phi \sim 0$  is not zero, as expected by absorption due to pair production prediction. Therefore, pair production is insufficient on its own to explain the observations: cascading and anisotropic inverse Compton scattering are also involved in the process (Dubus et al. 2008).

*Cascades:* The  $e^+e^-$  pair created when a stellar photon and a VHE photon interact has one of the particles carrying away most of the energy along the path of the  $\gamma$ -ray photon. This particle can upscatter stellar photons to VHE, even if lower than the initial VHE photon. The new  $\gamma$ -ray photon produces a pair again, triggering a cascade that stops when the upscattered photon energy is below the pair production threshold. Cascade emission reduces the effective opacity by redistributing the absorbed flux. This effect will probably be important only when the opacity is high and the source is behind the star, the case at periastron in LS 5039.

Emission and absorption processes are anisotropic and depend on the location because the pairs diffuse according to the local magnetic field properties. Pair emission can be confined to the place of their creation if their Larmor radius is very small compared with the system size (Dubus 2013). In this case, the pairs radiate locally the second  $\gamma$ -ray emission. In the case of low magnetic field, the spatial diffusion of the pairs cannot be neglected, making the problem rather intricate. When the magnetic field is high ( $\geq 5$  G), synchrotron starts to dominate the radiative losses of the pairs. For a field  $\geq 100$  G the cascade is stopped at the first generation of pairs. In this case, the VHE  $\gamma$ -rays are completely absorbed, in contrast with the observations. Therefore, if the magnetic field is high the VHE  $\gamma$ -ray photons have to be produced away from the compact object.

*Anisotropic inverse Compton scattering:* The  $\gamma$ -ray emission from LS 5039 is thought to be due to inverse Compton scattering. Because of the dependency of the Compton cross-section on angle between incoming and outgoing photons, an anisotropic distribution

of seed photons will lead to anisotropic emission from an isotropic distribution of electrons. Therefore, the emission from electrons upscattering stellar photons will be maximum directly towards the star, corresponding to head-on collisions, and minimum directly away from the star, tail-on collisions. Anisotropic inverse Compton scattering leads to an orbital modulation of the  $\gamma$ -ray lightcurve even for a constant acceleration of electrons. Therefore, in addition to  $\gamma\gamma$  absorption and cascading a variable intrinsic VHE  $\gamma$ -ray flux should be considered.

## V. CONCLUSIONS

In  $\gamma$ -ray binaries the VHE  $\gamma$ -rays can be absorbed by stellar photons to produce pairs. This leads to an orbital modulation that can be compared with observations. We have written a Fortran code to calculate the integral of the opacity of the absorption due to pair production, using the trapezoidal method and considering the point-like approximation for the massive star, for the binary system LS 5039. The results obtained for a system inclination  $i = 60^\circ$  show the minimum absorption near inferior conjunction, and the maximum near the periastron. Comparing with the results obtained by Dubus (2006), where the massive star size is considered, the only difference is seen for 10 TeV at  $\phi \sim 0$ . When the star size is considered, the energy threshold depends on the star region considered. This, globally, produces a reduction of the threshold and therefore, higher absorption. The results have been compared with the H.E.S.S lightcurve and we have seen that the absorption due to pair production is insufficient to explain the observations. It is necessary to involve processes like cascading or to assume that the VHE emission is produced away from the compact object.

## Acknowledgments

First, I would like to thank my advisor, Marc Ribó, for spending many hours with this project. In addition, I would like to thank my boyfriend, my sister and my mother for their patience during all the project.

- 
- [1] Aharonian, F., Akhperjanian, A. G., Aye, K.-M., et al. 2005a, A&A, 442, 1
  - [2] Aharonian, F., Akhperjanian, A. G., Aye, K.-M., et al. 2005b, Science, 309, 746
  - [3] Aharonian, F., Akhperjanian, A. G., Bazer-Bachi, A. R., et al. 2006, A&A, 460, 743
  - [4] Aharonian, F., Akhperjanian, A. G., et al. 2007, A&A, 469, L1
  - [5] Albert, J., Aliu, E., Anderhub, H., et al. 2006, Science, 312, 1771
  - [6] Casares, J., Ribó, M., Ribas, I., et al. 2005, MNRAS, 364, 899
  - [7] Dubus, G. 2006, A&A, 451, 9
  - [8] Dubus, G., Cerutti, B., & Henri, G. 2008, A&A, 477, 691
  - [9] Dubus, G. 2013, A&ARv, 21, 64
  - [10] Fermi LAT Collaboration, Ackermann, M., Ajello, M., et al. 2012, Science, 335, 189
  - [11] Gould, R. J., & Schröder, G. P. 1967, Phys. Rev., 155, 1404
  - [12] Moldón, J., Ribó, M., & Paredes, J. M. 2012, A&A, 548, A103
  - [13] Nikishov, A. I. 1962, Soviet Phys., 14, 393
  - [14] Paredes, J. M., Martí, J., Ribó, M., & Massi, M. 2000, Science, 288, 2340